



El Nino on the Devil's Staircase: Annual Subharmonic Steps to Chaos

Fei-Fei Jin; J. David Neelin; Michael Ghil

Science, New Series, Vol. 264, No. 5155 (Apr. 1, 1994), 70-72.

Stable URL:

<http://links.jstor.org/sici?sici=0036-8075%2819940401%293%3A264%3A5155%3C70%3AENOTDS%3E2.0.CO%3B2-G>

Science is currently published by American Association for the Advancement of Science.

Your use of the JSTOR archive indicates your acceptance of JSTOR's Terms and Conditions of Use, available at <http://www.jstor.org/about/terms.html>. JSTOR's Terms and Conditions of Use provides, in part, that unless you have obtained prior permission, you may not download an entire issue of a journal or multiple copies of articles, and you may use content in the JSTOR archive only for your personal, non-commercial use.

Please contact the publisher regarding any further use of this work. Publisher contact information may be obtained at <http://www.jstor.org/journals/aaas.html>.

Each copy of any part of a JSTOR transmission must contain the same copyright notice that appears on the screen or printed page of such transmission.

JSTOR is an independent not-for-profit organization dedicated to creating and preserving a digital archive of scholarly journals. For more information regarding JSTOR, please contact jstor-info@umich.edu.

- and event 37 for events on the west bank. All the masters were recorded by more than 500 stations.
10. A. Douglas, R. C. Lilwall, J. B. Young, *Atomic Weapons Research Establishment Report O 28/74 MOD Procurement Exec.* (Her Majesty's Stationary Office, London, 1972).
 11. A. M. Dziewonski, G. Ekstrom, J. E. Franzen, J. H. Woodhouse, *Phys. Earth Planet. Inter.* **45**, 1 (1987).
 12. ———, *ibid.* **66**, 133 (1991).
 13. ———, *ibid.* **67**, 210 (1991).
 14. Geological Survey of Sudan, *Geological Map of the Sudan* (scale 1:2,000,000) (Geological and Mineral Resources Department, Khartoum, Sudan, 1981).
 15. A. Holmes, *Geogr. J.* **48**, 149 (1916).
 16. C. H. Stigand, *ibid.*, p. 145.
 17. R. Gaulon, J. Chorowicz, G. Vidal, B. Romanowicz, G. Roult, *Tectonophysics* **209**, 87 (1992).
 18. H. E. Hurst and P. Phillips, *General Description of the Basin, Meteorology, Topography of the White Nile Basin*, vol. 1 of *The Nile Basin* (Government Press, Cairo, Egypt, 1931).
 19. War Office, *Juba Zone G Topographic Map Sheet N.B. 36/4* (scale 1:500,000) (Geographical Section General Staff No. 4355, Sudan, 1947).
 20. N. N. Ambreys and R. D. Adams, *Bull. Seismol. Soc. Am.* **76**, 483 (1986).
 21. B. Gutenberg and C. F. Richter, *Seismicity of the Earth* (Princeton Univ. Press, Princeton, NJ, 1954).
 22. We thank P. Davis, A. Douglas, J. Young, D. Jackson, J. Heirtzler, and D. Morgan for assistance and the Atomic Weapons Research Establishment Seismological Research Unit (Blacknest, United Kingdom), International Seismological Centre (Newbury, United Kingdom), the Department of Earth and Space Sciences at the University of California, Los Angeles (California), NASA/Goddard Space Flight Center (Greenbelt, Maryland), and the Geography Department at the University of Durham (Durham, United Kingdom) for logistical support.

28 September 1993; accepted 24 January 1994

El Niño on the Devil's Staircase: Annual Subharmonic Steps to Chaos

Fei-Fei Jin, J. David Neelin,* Michael Ghil

The source of irregularity in El Niño, the large interannual climate variation of the Pacific ocean-atmosphere system, has remained elusive. Results from an El Niño model exhibit transition to chaos through a series of frequency-locked steps created by nonlinear resonance with the Earth's annual cycle. The overlapping of these resonances leads to the chaotic behavior. This transition scenario explains a number of climate model results and produces spectral characteristics consistent with currently available data.

El Niño, the name given by Peruvian fishermen to an aperiodic warming of equatorial surface waters—now known to affect much of the globe (1)—refers to the Christ child because in years when it occurs, coastal manifestations tend to appear around Christmas. A decade of research has led to a view of El Niño as an essentially cyclic phenomenon and to an understanding of the mechanisms that drive the oscillation between warm and cold phases and determine the spatial pattern (2, 3). Current major theoretical challenges are the interaction of El Niño with the seasonal cycle (2), which provided its saintly name, and the source of its devilishly irregular behavior. We as well as Tziperman and colleagues (4) show how the latter is caused by the former. The respective approaches complement each other because Tziperman and co-workers analyze the basics of the mechanism in a simple model, while our model

provides fuller physical mechanisms, along with connections to other models. Our coupled ocean-atmosphere model (5, 6) is closely related to the Cane-Zebiak model used for operational predictions of El Niño (7). Ours has been used (5) to understand the relation among the flow regimes of many El Niño models (7–14) including complex coupled general circulation models and hybrid coupled models. This modeling pedigree is important because some earlier results on El Niño irregularity have arisen from numerical artifacts (15).

When the annual cycle is absent in El Niño models, the spatial pattern and inherent period of the interannual oscillations are determined by the nonlinear saturation of an oscillatory, unstable ocean-atmosphere mode. The instability involves feedbacks between the sea surface temperature (SST), which affects the atmospheric circulation, and the dynamics of the ocean circulation, in which currents and thermocline depth must adjust to the changes in wind. The resulting SST–ocean-dynamics modes have several regimes of behavior (3), mirrored in the differing behavior of several climate models (12). Observational evidence (16, 17) points to a regime in which the memory of the system is provided mainly by the time scale of subsurface adjust-

ment by ocean dynamics, whereas the spatial form and growth mechanisms are largely independent of these time scales. The large spatial scale of El Niño and its atmospheric manifestation, the Southern Oscillation (together known as ENSO), arise because each medium responds in an integrating fashion to the anomalies of the other, favoring the growth of the largest scale mode. The oscillatory behavior occurs because the slowly adjusting ocean dynamics never quite catch up with the changes in the wind over the basin. A convenient metaphor for this process is known as the delayed-oscillator model (4, 9, 13). This simple model, with idealized wind anomalies depending on SST at a single point and truncated ocean dynamics, can be justified in terms of the mixed SST–ocean-dynamics modes of more complex models [see (3) for review] for significant portions of their respective bifurcation diagrams (5).

When the seasonal cycle is included in a coupled model with El Niño oscillations and no atmospheric noise, several things can happen: The motion can be quasiperiodic (that is, with two incommensurable frequencies, the inherent El Niño frequency and its annual modulation); the motion can be irregular; or the El Niño cycle can be entrained nonlinearly into synchrony with the annual cycle to form a periodic oscillation with a longer period—a subharmonic oscillation. We mapped this interaction of El Niño and the seasonal cycle systematically in our model and found it to be organized about a “devil's staircase”—a structure in which the inherent frequency of the system locks onto a sequence of rational fractions of the external frequency and that is associated with the transition to chaos by the overlapping of these nonlinear resonances (18).

The approximate devil's staircase in Fig. 1A is constructed from many 100-year runs of the model. We changed a parameter, δ_s , which determines the strength of anomalous currents and upwelling in the model's surface layer (5), to modify the inherent period of the model El Niño cycle. For stronger surface-layer feedbacks, zonal and vertical advection anomalies add to the time rate of change of SST caused by thermocline-depth anomalies. The most realistic regime for the model ENSOs occurs between values of about 0.2 and 0.4 on this nondimensional scale. We swept through a greater range of values to see the structure in which the realistic range is embedded, and because some climate models fall into the higher value range (12). Over much of the parameter range, the ENSO frequency is discretized into a series of frequency-locked steps (known as Arnold tongues) at rational fractions of the annual frequency. A complete devil's staircase has an infinite

F.-F. Jin, Department of Meteorology, University of Hawaii at Manoa, Honolulu, HI 96822, USA.

J. D. Neelin, Department of Atmospheric Sciences, University of California at Los Angeles, Los Angeles, CA 90024–1565, USA.

M. Ghil, Department of Atmospheric Sciences and Institute of Geophysics and Planetary Physics, University of California at Los Angeles, Los Angeles, CA 90024–1565, USA.

*To whom correspondence should be addressed.

number of steps, filling the parameter range; for the staircase of Fig. 1A, we found a large number of these steps as we roughly followed the critical surface (18) where the complete staircase would appear. This route to chaos fundamentally involves two parameters: one affecting the inherent ENSO frequency and the other controlling the strength of ocean-atmosphere feedbacks. The first, δ_s , gives rise to the steps; the second, the coupling parameter μ (5), increases their width as the nonlinear effects become stronger. Some steps, notably that for 4-year locking, widen rapidly as μ increases (Fig. 1B) (19).

As we increased μ for a fixed δ_s , the model passed first from a stable annual cycle with no ENSO to a quasiperiodic regime in which the ENSO frequency is not locked and then to a frequency-locked regime. The qualitative behavior of the time series for these successive regimes supports the results presented by Tziperman and colleagues (4) for a simpler model. For example, Fig. 2 shows the final transition for a case that lies close to the right edge of the 5-year locked

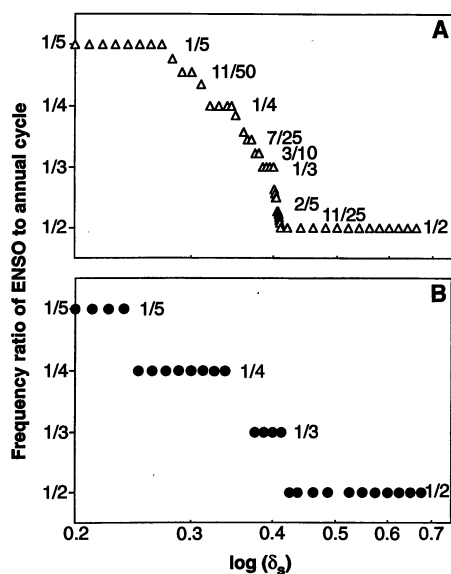


Fig. 1. Frequency ratio of the model El Niño oscillation to the annual cycle, as a function of a parameter, δ_s , that affects the inherent ENSO period. Another parameter, the coupling coefficient, μ , is changed to keep the El Niño cycle below its transition to chaos. Nonlinear frequency locking to the annual cycle creates a staircase of discrete steps at rational values of the frequency ratio. For instance, for a frequency ratio 1/4, the ENSO period is exactly 4 years, while for 3/10, a sequence of three El Niño cycles repeats every 10 years. (A) The approximate devil's staircase, slightly above the primary Hopf bifurcation where the ENSO mode goes unstable. All points shown correspond to rational frequency ratios (some labeled). (B) Frequency-locked solutions for slightly larger (by about 10%) values of μ , showing the rapid widening of the integer-period steps.

step of Fig. 1A. For slightly larger coupling, the ENSO signal locked to a 4-year period (Fig. 1B): The spectrum (Fig. 2A) exhibits quadrennial and annual peaks, plus secondary peaks at biennial periods and 4/3 of a year periods produced by the nonlinear interaction of the two main frequencies. As μ was increased further, the width of the steps broadened, and chaos ensued as the system jumped between them (Fig. 2B). The broadband spectrum is a signature of deterministic chaos, but the peaks corresponding to the nonlinear resonances may still be detected.

The anomalous SSTs corresponding to the case of Fig. 2B (Fig. 3) vary essentially as a standing oscillation with a time scale determined by subsurface dynamical adjustment, consistent with ENSO observations and several other ENSO models. Comparison to the linear stability analysis of the periodic basic state (20) shows that the spatial pattern of the nonlinear, chaotic variability is dominated by the unstable mode that creates the bifurcation to the El Niño cycle. This mode has the same essential dynamics when the seasonal cycle is present as without it. The interactions of this ENSO mode with the annual cycle occur primarily through the equatorial upwelling and thermocline slope, which are modulated by seasonal wind stress variations (2). Both upwelling and thermocline depth affect the way that changes in ocean circulation resulting from earlier SST and wind anomalies translate, at later stages of the cycle, into warming or cooling of SST in the crucial equatorial region. This relation makes it easier for coupled feedbacks to produce an SST anomaly at certain times of

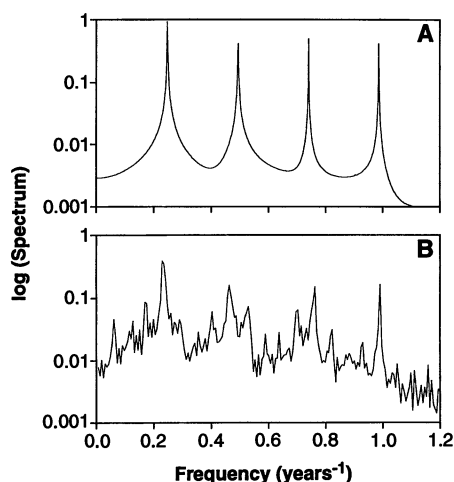


Fig. 2. Power spectra of eastern Pacific equatorial SST (averaged from 135°W to 90°W) from the last 500 years of two 520-year model integrations (bandwidth of 0.06 year⁻¹). (A) For a case of frequency locking to 4-year period. (B) For a case with a slightly higher value of the coupling parameter, μ , which exhibits chaotic behavior.

year, notably winter, thus tending to delay or advance the phase of the El Niño slightly to match the favorable season.

A test of this scenario is whether the subharmonic peaks associated with the nonlinear resonances are observed in data. A period-doubling route to chaos would not have the quasi-quadrennial peak larger than the quasi-biennial peak (21), and irregularity created by stochastic forcing alone would not likely have multiple interannual peaks, given the properties of the annual average problem (5). Additional irregularity associated with atmospheric stochastic forcing can significantly increase the red background in the signal and make the peaks harder to detect but would not change the basic scenario. Observational studies (22, 23) do show multiple spectral peaks in ENSO time series, although the records are admittedly short. Rasmusson and colleagues (22) resolved a quasi-biennial and a lower frequency 3- to 6-year peak. Jiang and co-workers (23) corroborated this split of the ENSO variability and found that the low-frequency peak was quasi-quadrennial; this peak dominates ENSO-related variance, with a smaller quasi-biennial contribution. Several studies (17, 23, 24) have shown that the two main ENSO time scales have similar spatial structures, also in agreement with our scenario.

This scenario for El Niño chaos accounts for seemingly diverse results from ENSO modeling of the past decade. For instance, a number of model simulations have been disappointingly regular, because of frequency locking to the seasonal cycle (9, 11); excessive locking can present a significant barrier to the accuracy of El Niño forecasts. In our

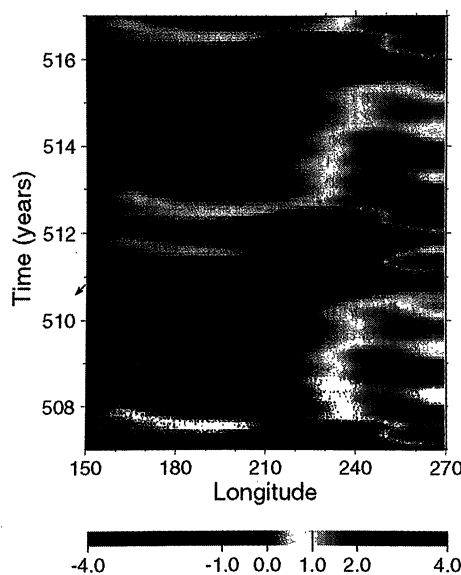


Fig. 3. Time-longitude plot of Pacific SST anomalies along the equator, for a typical 10-year interval from the model run corresponding to Fig. 2B.

scenario, these models are stuck on one of the steps of the staircase, partway along the transition to irregular behavior. Furthermore, these results show how a large body of modeling and theory on simpler versions of ENSO carries over to the case of complex behavior: The basic characteristics of El Niño do not depend on the seasonal cycle—but its chaotic behavior does.

REFERENCES AND NOTES

1. E. M. Rasmusson and T. H. Carpenter, *Mon. Weather Rev.* **110**, 354 (1982); M. A. Cane, *Science* **222**, 1189 (1983); E. M. Rasmusson and J. M. Wallace, *ibid.*, p. 1195; S. G. H. Philander, *Nature* **302**, 295 (1983).
2. S. G. H. Philander, *El Niño, La Niña, and the Southern Oscillation* (Academic Press, San Diego, CA, 1990).
3. J. D. Neelin, M. Latif, F.-F. Jin, *Annu. Rev. Fluid Mech.* **26**, 617 (1994).
4. E. Tziperman, L. Stone, M. A. Cane, H. Jarosh, *Science* **264**, 72 (1994).
5. F.-F. Jin and J. D. Neelin, *J. Atmos. Sci.* **50**, 3477 (1993); J. D. Neelin and F.-F. Jin, *ibid.*, p. 3504; F.-F. Jin and J. D. Neelin, *ibid.*, p. 3523.
6. The model of (5) has been modified to include the observed seasonal heat flux and wind stress [F.-F. Jin, J. D. Neelin, M. Ghil, *Proceedings of the Ninth Conference on Atmospheric and Oceanic Waves and Stability*, San Antonio, TX, 10 to 14 May 1993 (American Meteorological Society, Boston, 1993)].
7. M. A. Cane and S. E. Zebiak, *Science* **228**, 1084 (1985); S. E. Zebiak and M. Cane, *Mon. Weather Rev.* **115**, 2262 (1987); M. Cane, S. E. Zebiak, S. C. Dolan, *Nature* **321**, 827 (1986); T. Barnett *et al.*, *Science* **241**, 192 (1988).
8. P. S. Schopf and M. J. Suarez, *J. Atmos. Sci.* **45**, 549 (1988); Y. Wakata and E. S. Sarachik, *ibid.* **48**, 2060 (1991).
9. D. S. Battisti and A. C. Hirst, *ibid.* **46**, 1687 (1989).
10. S. G. H. Philander, R. C. Pacanowski, N. C. Lau, M. J. Nath, *J. Clim.* **5**, 308 (1992); N. C. Lau, S. G. H. Philander, M. J. Nath, *ibid.*, p. 284; P. R. Gent and J. J. Tribbia, *ibid.* **6**, 1843 (1993); G. A. Meehl, *ibid.* **3**, 72 (1990); T. Nagai, T. Tokioka, M. Endoh, Y. Kitamura, *ibid.* **5**, 1202 (1992); M. Latif, A. Sterl, E. Maier-Reimer, M. M. Junge, *ibid.* **6**, 5 (1993).
11. D. L. T. Anderson and J. P. McCreary, *J. Atmos. Sci.* **42**, 615 (1985); T. P. Barnett *et al.*, *J. Clim.* **6**, 1545 (1993); H.-H. Syu, J. D. Neelin, W. Weibel, D. Gutzler, *Extended Abstract Volume, Fourth Symposium on Global Change Studies*, Anaheim, CA, 17 to 22 January 1993 (American Meteorological Society, Boston, 1993); D.-H. Wu, D. L. T. Anderson, M. K. Davey, *J. Clim.* **6**, 1703 (1993).
12. J. D. Neelin *et al.*, *Clim. Dyn.* **7**, 73 (1992).
13. M. J. Suarez and P. S. Schopf, *J. Atmos. Sci.* **45**, 3283 (1988).
14. M. Münnich, M. Cane, S. E. Zebiak, *ibid.* **48**, 1238 (1991).
15. G. K. Vallis, *Science* **232**, 243 (1986); G. K. Vallis, *J. Geophys. Res.* **93**, 13979 (1988).
16. N. E. Graham and W. B. White, *Science* **240**, 1293 (1988).
17. M. Latif, A. Sterl, E. Maier-Reimer, M. M. Junge, *J. Clim.* **6**, 700 (1993).
18. M. H. Jensen, P. Bak, T. Bohr, *Phys. Rev. A* **30**, 1960 (1984); P. Bak, *Phys. Today* **1986**, 38 (December 1986); ——— and R. Bruinsma, *Phys. Rev. Lett.* **49**, 249 (1982); D. G. Aronson, M. A. Chory, G. R. Hall, R. P. McGehee, *Commun. Math. Phys.* **83**, 303 (1982); M. J. Feigenbaum, L. P. Kadanoff, S. J. Schenker, *Physica D* **5**, 370 (1982).
19. In Fig. 1A, we varied μ with δ_s to keep the system in the range in which a large number of Arnold tongues may be detected; this range lies quite close to the primary bifurcation. The detection of additional tongues is easier in cases with

- a reduced amplitude of the annual cycle, where the steps widen less rapidly with μ .
20. With the use of Floquet theory [for example, G. Iooss and D. D. Joseph, *Elementary Stability and Bifurcation Theory* (Springer-Verlag, New York, 1990); see (6)].
 21. M. J. Feigenbaum, *J. Stat. Phys.* **19**, 25 (1978); B. Legras and M. Ghil, *J. Méc. Théor. Appl.*, numéro spécial, 45 (1983).
 22. E. M. Rasmusson, X. Wang, C. F. Ropelewski, *J. Mar. Syst.* **1**, 71 (1990); C. L. Kepenne and M. Ghil, *J. Geophys. Res.* **97**, 20449 (1992).
 23. N. Jiang, J. D. Neelin, M. Ghil, *Proceedings of the*

- 17th Climate Diagnostics Workshop*, Norman, OK, 19 to 23 October 1992 (Climate Analysis Center, Washington, DC, 1993).
24. T. P. Barnett, *J. Clim.* **4**, 269 (1991).
 25. We thank J. Weiss for useful references and W. Weibel for graphics. Supported in part by National Science Foundation grants ATM-9215090, ATM-9013217, and ATM-9312888; National Oceanic and Atmospheric Administration grant NA26GP0114-01; and Digital Equipment Corporation grant 1243.

29 October 1993; accepted 31 January 1994

El Niño Chaos: Overlapping of Resonances Between the Seasonal Cycle and the Pacific Ocean-Atmosphere Oscillator

Eli Tziperman,* Lewi Stone, Mark A. Cane, Hans Jarosh

The El Niño–Southern Oscillation (ENSO) cycle is modeled as a low-order chaotic process driven by the seasonal cycle. A simple model suggests that the equatorial Pacific ocean-atmosphere oscillator can go into nonlinear resonance with the seasonal cycle and that with strong enough coupling between the ocean and the atmosphere, the system may become chaotic as a result of irregular jumping of the ocean-atmosphere system among different nonlinear resonances. An analysis of a time series from an ENSO prediction model is consistent with the low-order chaos mechanism.

El Niño (roughly defined as the warming of the east equatorial water of the Pacific Ocean about every 3 to 6 years) and the accompanying Southern Oscillation signal in the atmosphere dramatically affect the Earth's climate on a global scale. The onset, termination, and cyclic nature of the ENSO events seem to be well explained by the linear equatorial wave dynamics and the delay oscillator idea (1–5). However, their irregular occurrence and partial locking to the regular seasonal cycle [El Niño events usually peak in the northern winter (6)] have been difficult to explain.

Here we use a simple delay equation model, including idealized seasonal forcing, to evaluate whether ENSO might be a low-order chaotic process driven by the seasonal cycle. We then analyze the chaotic behavior of the ENSO model of Cane and Zebiak [(7), hereafter CZ]. A companion paper (8) describes another test of this theory that uses a model that is fuller than our simple delay model and yet simpler (and therefore more accessible) than the CZ model from which we analyze a time series here.

The delay oscillator mechanism can be described as follows: A positive sea-surface temperature (SST) perturbation along the

eastern equatorial Pacific weakens the easterly winds above the equator [the Bjerknes hypothesis (9)]. The change in the winds excites a downwelling (deepening) wave in the thermocline that travels eastward to the South American coast as equatorial Kelvin waves and an upwelling signal that travels westward as equatorial Rossby waves. The downwelling Kelvin waves enhance the warming off the coast of South America—the El Niño event has begun. Subsequently, the westward-traveling upwelling Rossby waves are reflected from the western boundary of the Pacific Ocean as upwelling Kelvin waves, which travel eastward to counter the downwelling Kelvin waves, ultimately terminating the El Niño event.

We used a simple heuristic model of this accepted delay mechanism, including a Kelvin wave, one Rossby wave mode, and a dynamic link from mid-Pacific wind stress anomalies to these equatorial wave modes. To these we added a phenomenological seasonal forcing term representing the effects of the numerous seasonally varying features of the equatorial Pacific ocean and atmosphere, such as wind amplitude and SST variations (10). Apart from the seasonal forcing term used here, our model is basically a continuous version of the discrete delay equation given in (5) and is similar to those of (1–4). The equation is written for $h(t)$, the thermocline depth deviations from seasonal depth values at the eastern boundary

E. Tziperman, L. Stone, H. Jarosh, Environmental Sciences and Energy Research, The Weizmann Institute of Science, Rehovot 76100, Israel.
M. A. Cane, Lamont-Doherty Earth Observatory, Columbia University, Palisades, NY 10964, USA.

*To whom correspondence should be addressed.